

# SUPPORTING INFORMATION

## Sensitive Analysis of Protein Adsorption to Colloidal Gold by Differential Centrifugal Sedimentation

Adam M. Davidson,<sup>†</sup> Mathias Brust,<sup>†</sup> David L. Cooper,<sup>†</sup> and Martin Volk<sup>\*,‡</sup>

<sup>†</sup> Department of Chemistry, Crown Street, University of Liverpool, Liverpool L69 7ZD, UK.

<sup>‡</sup> Surface Science Research Centre, Department of Chemistry, Abercromby Square, University of Liverpool, Liverpool L69 3BX, UK.

### Table of Contents

<b>S1. UV-vis Spectra</b> .....	<b>S2</b>
<b>S2. Size Distributions Measured Without BSA in the DCS-Gradient Fluid</b> .....	<b>S3</b>
<b>S3. Effect of Uncertainty of the Value of the Corona Density <math>\rho_{\text{Prot}}</math></b> .....	<b>S4</b>
<b>S4. Fits of Adsorption Isotherms</b> .....	<b>S5</b>
<b>References</b> .....	<b>S6</b>

All raw data are openly available from the University of Liverpool Research Data Catalogue at DOI: [10.17638/datacat.liverpool.ac.uk/242](https://doi.org/10.17638/datacat.liverpool.ac.uk/242).

## S1. UV-vis Spectra

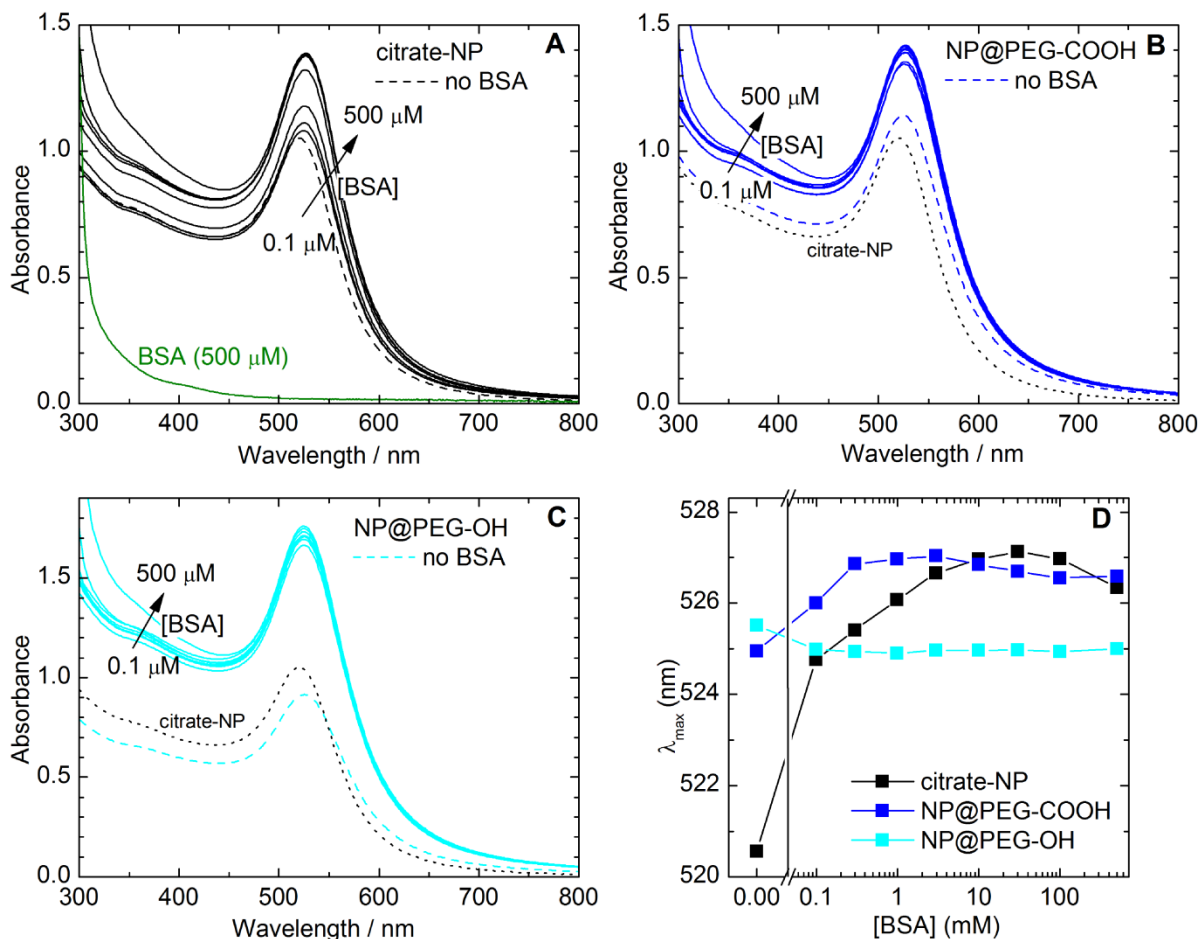


**Figure S1.** UV-Vis absorbance spectra of citrate- (A) and different PEG-stabilized (B,C) gold NPs, before (dashed lines) and after (solid lines) protein corona formation by incubation for 24 hours in BSA solutions of different concentrations, as indicated. The data shown here were measured in the presence of BSA. Spectra of NPs before incubation in BSA solution were not measured at the same NP concentration as spectra after incubation. For comparison, (A) also shows the spectrum of a solution of BSA at high concentration. (D) Variation of the center position of the plasmon resonance band,  $\lambda_{\max}$ , with the concentration of BSA used during incubation, as determined from the spectra shown in (A) - (C), using fits of the plasmon resonance band with an unsymmetric Voigt function.

## S2. Size Distributions Measured Without BSA in the DCS-Gradient Fluid

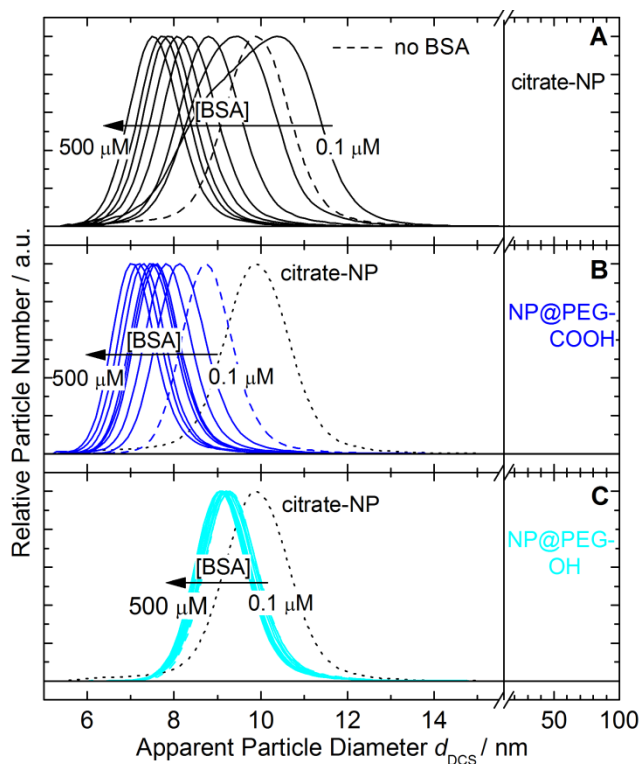


**Figure S2.** Size distributions for citrate- (A) and different PEG-stabilised (B,C) gold NPs, before (dashed lines) and after (solid lines) protein corona formation by incubation for 24 hours in BSA solutions of different concentrations, as indicated. The data shown here were obtained without BSA in the DCS-gradient fluid. The dotted lines in panels B and C show the distribution of citrate-stabilized NPs in the absence of BSA or other ligands.

### S3. Effect of Uncertainty of the Value of the Corona Density $\rho_{\text{Prot}}$

As discussed in the main text, a value of  $\rho_{\text{Prot}} = 1.15 \text{ g/cm}^3$  is assumed for the analysis of DCS data. The possible variation of this value within a reasonable range (1.1-1.2  $\text{g/cm}^3$ ) leads to an uncertainty of the reported value of the corona thickness  $s_{\text{Prot}}$  which can be calculated using Eqns. (2) - (4), see Fig. S3. For a given experimental result  $d_{\text{DCS}}$ , the actual corona thickness  $s_{\text{Prot}}$  can be read directly from these figures, as indicated by the dotted lines. It is obvious that for thin capping layers, the exact value of the corona density does not greatly affect the result. However, as the capping layer approaches the dimensions of the gold core, the value of the corona density increasingly affects the result. For the highest BSA concentrations, the results suffer from some uncertainty due to the uncertainty in the value of  $\rho_{\text{Prot}}$ , as indicated by the red lines. This is particularly pronounced for NPs with a PEG-capping layer, since for these NPs the total organic capping layer (PEG + protein corona) is significantly thicker than for the citrate-stabilized NPs.

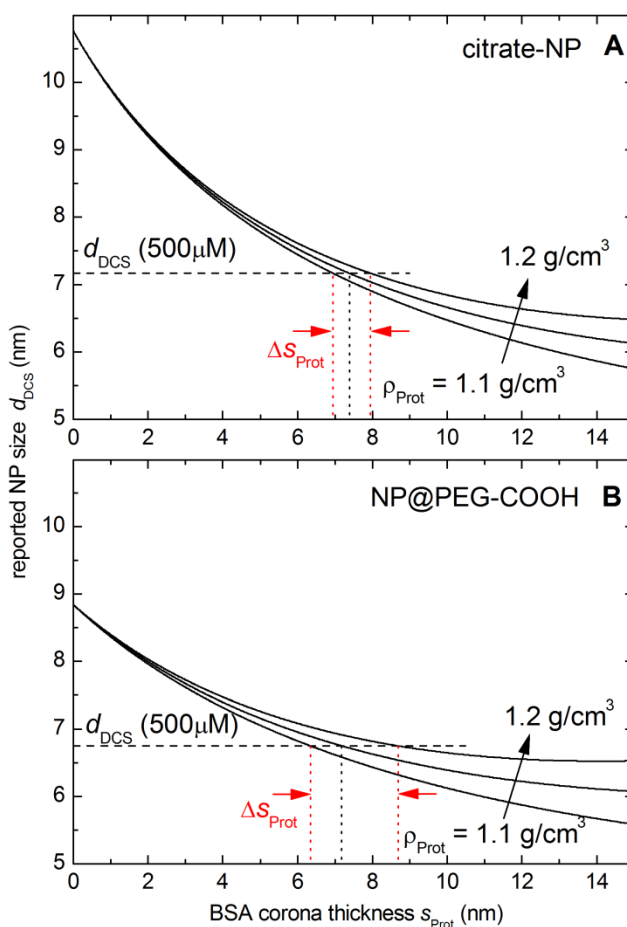


**Figure S3.** NP diameter which would be reported by the DCS software for different corona thicknesses  $s_{\text{Prot}}$  and densities  $\rho_{\text{Prot}}$  (1.1, 1.15, 1.2  $\text{g/cm}^3$ ) for citrate-stabilized NPs (A, Eqns. (2) and (4) of the main text, using  $d_{\text{AU}} = 10.8 \text{ nm}$ ) and NP@PEG-COOH (B, Eqns. (3) and (4), using  $d_{\text{AU}} = 10.8 \text{ nm}$  and  $s_{\text{PEG-COOH}} = 3.0 \text{ nm}$ ). Horizontal dashed lines indicate the experimental values for  $[\text{BSA}] = 500 \mu\text{M}$  and vertical dotted lines the corona thickness which is calculated for  $\rho_{\text{Prot}} = 1.15 \text{ g/cm}^3$  (black) and 1.1 or 1.2  $\text{g/cm}^3$  (red). The uncertainties of  $s_{\text{Prot}}$  in Fig. 2 are half of the values  $\Delta s_{\text{Prot}}$  indicated here.

## S4. Fits of Adsorption Isotherms

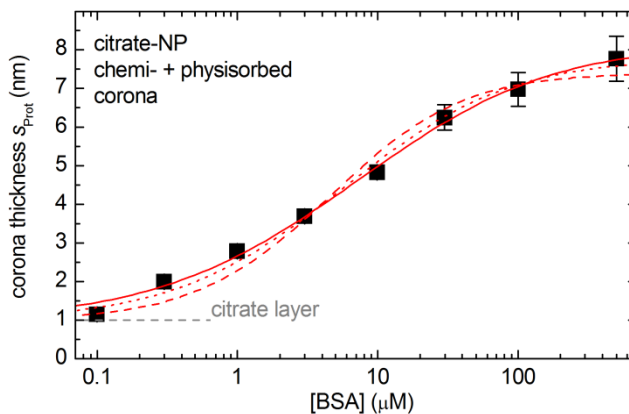


**Figure S4.** BSA corona thickness on citrate-stabilized NPs after incubation at different BSA concentrations for 24 hours, determined from DCS-measurements with BSA present in the gradient fluid at the same concentration as during NP incubation, *i.e.* chemi- and physisorbed corona. The solid red line is a fit of the data to the Hill model, (Eqns. 5 and 6), yielding values of  $s_{\text{max}} = (8.2 \pm 0.3)$  nm,  $K_D = (22 \pm 7)$   $\mu\text{M}$  and  $n = 0.69 \pm 0.05$ , the dashed red line is a fit of the data to a Langmuir isotherm (Eqns. 5 and 6 with  $n = 1$ ), yielding a binding constant of  $K_D = (9.6 \pm 2.4)$   $\mu\text{M}$ . For further showing the sensitivity of the Hill binding constant to the exact value of  $n$ , the dotted line shows a fit to the Hill model with  $n$  fixed to 0.8, yielding a binding constant of  $K_D = (14.6 \pm 2.4)$   $\mu\text{M}$ . We note that, given the complexity of the effect, with two very different binding modes operating in parallel, this model is not appropriate, but the fits allow comparison with previous results in the literature. In particular, we note the similarity of these fit results with those reported recently for BSA binding to 12.6 nm gold NPs using using AUC.<sup>1</sup> On the other hand, significantly stronger anti-cooperativity ( $n = 0.4$ ) and higher binding constants ( $K_D = 250$   $\mu\text{M}$ ) were reported for BSA binding to 51 nm gold NPs, based on PSCS data.<sup>2, 3</sup> We suggest that these different results are due to the larger uncertainty of those data which result in the fit converging to a low value of  $n$  which then artificially increases the value of  $K_D$ ; in fact, a fit of our data with a fixed value of  $n = 0.4$  also yields a dissociation constant of several 100  $\mu\text{M}$ , although this is a clearly unsatisfactory fit.

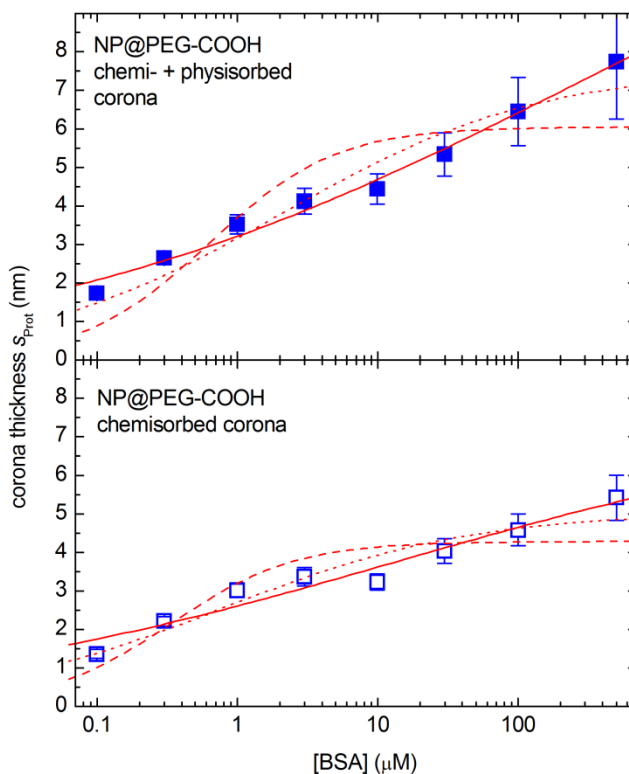


**Figure S5.** BSA corona thickness on NP@PEG-COOH after incubation at different BSA concentrations for 24 hours, determined from DCS-measurements with BSA present in the gradient fluid at the same concentration as during NP incubation, *i.e.* chemi- and physisorbed corona (solid symbols), or DCS-measurements without BSA in the gradient fluid (open symbols). The solid red lines are fits of the data to the Hill model, (Eqns. 5 and 6), yielding values of  $s_{\max} = (14 \pm 7)$  nm,  $K_D = (7000 \pm 34000)$   $\mu\text{M}$  and  $n = 0.26 \pm 0.05$  for the combined chemi- and physisorbed corona and  $s_{\max} = (7 \pm 3)$  nm,  $K_D = (140 \pm 730)$   $\mu\text{M}$  and  $n = 0.26 \pm 0.10$  for the chemisorbed corona alone. The errors reported by the fitting program reflect the high uncertainty of the fit values arising from the wide transition shown by these isotherms and we do not suggest that the values reported here are meaningful, but report them simply as phenomenological values for describing the isotherms. The dashed red lines are fits of the data to a Langmuir isotherm (Eqns. 5 and 6 with  $n = 1$ ), yielding a binding constant of  $K_D = (1.1 \pm 0.6)$   $\mu\text{M}$  for the combined chemi- and physisorbed corona and  $K_D = (0.5 \pm 0.25)$   $\mu\text{M}$  for the chemisorbed corona alone; clearly, these are completely unsatisfactory fits. As a further demonstration of the sensitivity of the Hill binding constant to the exact value of  $n$ , the dotted lines show fits to the Hill model with  $n$  fixed (arbitrarily) to 0.5, yielding a binding constant of  $K_D = (7 \pm 4)$   $\mu\text{M}$  for the combined chemi- and physisorbed corona and  $K_D = (2 \pm 1)$   $\mu\text{M}$  for the chemisorbed corona alone.

## References

- (1) Bekdemir, A.; Stellacci, F. *Nat. Commun.* **2016**, *7*, 13121.
- (2) Dominguez-Medina, S.; McDonough, S.; Swanglap, P.; Landes, C. F.; Link, S. *Langmuir* **2012**, *28*, 9131-9139.
- (3) Dominguez-Medina, S.; Blankenburg, J.; Olson, J.; Landes, C. F.; Link, S. *ACS Sustainable Chem. Eng.* **2013**, *1*, 833-842.